Al-Rafidain Engineering Journal (AREJ) Vol.27, No.2, September 2022,pp.127-139

Dynamic Simulation and Optimization of Flat Plate Solar Collector Parameters Using the MATLAB Program for Erbil-Iraq Climate Condition

Kamaran Fatah Rashid engkamaranmec@gmail.com
Idres Azzat Hamakhan idres.hamakhan@su.edu.krd
Chalang Hamarasheed Mohammed chalang.mohammed@su.edu.krd
Mechanical and Mechatronics Department, Collage of Engineering, University of Salahaddin, Erbil, Iraq

Received: 3/4/2022 Accepted: 31/7/2022

ABSTRACT

This research aims to investigate the performance of solar water collector by varying: mass flow rate, inclination angle, total solar radiation, pipe size, and number of glass covers. The test rig was established to collect the data for the whole months of September and October and use it as a focal point for analysis of the solar water heating system's performance. The dynamic behavior was simulated and optimized with M_{ATLAB} software for the practical data to investigate the performance of the flat plate solar collector. The novelty in this study is the first time the authors use the whole practical data instead of average data to approximate the theoretical dynamic investigation of the flat plate solar collector. The achievements are as follows: the collector's efficiency was increased from 62.17% to 71.26% when the collector pipe spacing was reduced from 186 mm to 86 mm; the increase in efficiency was approximately 2% as the collector pipeline diameter increased from 1 mm to 50 mm; the optimum efficiency was achieved with triple glazing and was about 0.83%; the mass flow rate increases from 1 to 5 liters per minute, so it improves the efficiency of the system from 64% to 83%. Moreover, the best tilt angle for the flat plate solar collector was 30°. Also, the heat loss coefficient was raised by around 50% when wind speed was increased from 1 m/s to 5 m/s. Thus, the use of dynamic investigation with actual data will assist the researchers in improving the performance of the solar water flat plate collector.

Keywords:

First keyword; Dynamic simulation, Solar energy, Collector efficiency, Performance analysis.

==========

1. INTRODUCTION

Nowadays, renewable energy is used in electricity production broadly. Renewable energy resources positively influence the world's environmental, economic, and political challenges. The entire installation capability of renewable energy sources accounted for 9% of total power output by the end of 2001. Subsequently, in 2017 the capacity of renewable energy sources worldwide increased to 2,195 GW, where solar-wind driving power had the majority of this expansion. However, using renewable energy in buildings and power plants still faces several difficulties. To address these issues, several nations are working to change their renewable energy policy via enforceable laws, financial incentives, and other support mechanisms [1- 2].

The necessity to develop solar energy as an alternative power has increased as the world's power sources have run out. Much research on solar energy's applications has been widely done due to its abundance, freedom, and environmental friendliness. Recently, solar energy was deployed to conserve 1383 kW of power annually. In addition, it is an environmental friend as it reduces the annual emissions of CO_2 of around 781 kg for every flat plate solar collector [3].

Solar collectors are classified as non-focused and focused [4]. The solar thermal collector flat plat seems to be the greatest prevalent kind of solar collector used in domestic solar liquid heaters for home warming and heated water processes [5].

Several tests and researches continue to be interested in improving the design and

optimizing the working environments of a flat solar collector. These studies assessing the qualities of such devices, the design and the potential user must evaluate several aspects. The primary categories are thermal efficiency, cost and longevity, durability, upkeep, and simplicity of installation. The collector's performance can be improved when heat losses are minimized and the output temperature is raised as much as possible [6].

Several studies [6, 7] have been conducted in designing collector solar hot water systems, thermal performance appraisal, and optimization. In reference [6], the collector's total loss coefficient under various numbers and types of covers was studied. Also, adding more covers to FPSC reduces the top heat loss. This performance improvement is made by mixing Plexiglas and glass.

Cooper [8] investigated the effect of a collector's inclination angle relative to the horizontal mostly on the coefficient of heat losses. The overall heat loss coefficient increases somewhat with an angle of the inclination until a value is expected to be 60°, at which point the coefficient of heat losses increases dramatically. The impact of wind speed, number of glass covers, ambient temperature, gap space among glazing cover, absorber plate, inclination angle, and absorbers plate emissivity on a total loss of heat coefficient of flat plate collectors were investigated by Agbo and Okoroigwe [9].

These characteristics have been proven to impact the total heat losses within the collecting unit of the solar collectors' water heating systems. Ango et al. [7] investigated the influence of various operational and design factors on the act of the polymer flat plat solar collectors. This work revealed that extending the length of the polymer FPSC has no influence on a solar collector's achievement, but increasing an air gap width does, with an ideal performance achieved at such an air cavity width of roughly 10 millimeters, leading to an ideal performance. In addition, raising the flow rate enhances the efficiency of a polymer FPSC and lowers the coolant's exit temperature. The temperature of the inlet coolant has been proven to have a significant impact, mainly on polymer collector effectiveness. The input coolant's temperature must be at least equal to the ambient temperature for excellent performance.

The flat plate solar collectors are often evaluated in a steady state or quasi-stationary state [6, 10]. However, the weather in various regions of the world is insufficient for outside steady-state testing, which needs that keep the ambient temperature below particular parameters. Whereas it is difficult to attain steady state testing procedures, the dynamic test methodologies, considered in this paper as a good alternative for assessing the heat transfer performance of collectors, have been developed.

A dynamic response is a mathematical block diagram representing a process that depends on time-varying, namely a continuous system [11]. This dynamic behavior of flat plate-solar collectors has significant interest and is used to forecast the collector's time-dependent behavior under varying solar radiation intensity combined with weather situations. The dynamic evaluation method is used in analyzing specific solar panels by examining collector characteristics. This modeling is a guide to increase the efficiencies and minimize the cost function, which is used as an error term in the control system for certificate authorities.

Furthermore, the dynamic simulation and optimization of flat plate solar collectors by MATLAB software of any parameter has great importance in quality management and performance. The simulation and optimization are enhanced the solar collector in a short time and effectively solar collector producers.

Many research studies were found in the literature to assess a collector's transitory behavior [12, 13]. Understanding a solar collector's thermal behavior (or modeling) is crucial for predicting energy production annually. Thus, this modeling is acceptable for a solar thermal system to achieve suitable heat energy for practical experience.

In this research, a dynamic analysis approach and optimization for the solar collector parameters were investigated to generate thermal performance parameter estimations and increase collector efficiency.

This study aims to see how the liquid mass flow rate, inclination angle, total solar radiation, pipe size, and number of glass covers affect the performance of solar water collectors. To accomplish these goals, MATLAB software was employed.

This study presents, for the first time in Iraq-Erbil, the optimization of the most important parameters for the flat plate solar collector system, which in turn affects the improvement of the performance of this system.

2. MATERIALS AND METHODS

Figure 1 shows the design representation of a flat plate solar collector (FPSC) with water pipelines. A complete investigation of all collector heat losses is fundamental to obtaining a

total heat loss coefficient (conductance). The quantity of solar energy engrossed per the unit area of a plate is indicated by I_t at some representative place on an absorber plate where the temperature is Tp. This absorbed energy was split between losses at the top, rear, and edges as well as usable energy gain.

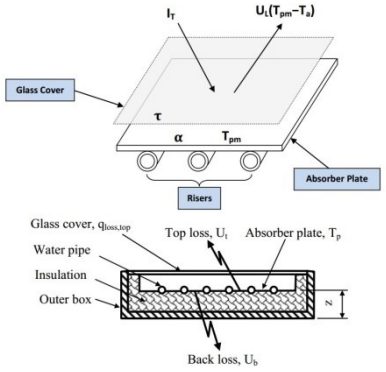

Fig.1 Shows schematic of the flat solar collector with liquid pipelines.

2.1. Flat-plate solar collector's heat transfer

The following relationship [14, 15] may be applied to represent the heat gated by the collector:

$$Q_c = F_R A_c[\alpha\tau I_t - U_L(T_{ci} - T_a)] \quad (1)$$

F_R = collector heat removal factor.
A_c = collector area m^2.
I_t = incident tatal solar radiation W/m^2.
U_L = top heat loss overall $W/m^2°C$.
α= absorptance.
τ = transmittance.
T_{ci} = collector water temperature at inlet °C.
T_a = temperature of ambient °C.

Usable Heat gain by the fluid Q_u.

$$Q_u = \dot{m}C_p(T_{co} - T_{ci}) \quad (2)$$

Where ṁ denotes the mass flow rate of the fluid in kg/s, Cp is the heat capacity of fluid in kJ/kg.°C, and Tco is the outlet water temperature of the collector in °C.

2.2. Systems of the solar heating thermal efficiency

The fraction of usable heat uptake by means of the collector to solar radiations on the absorber (η_c) is the collector efficiency of solar heating systems [16].

$$\eta_c = \frac{Q_u}{A_c I_t} \quad (3)$$

When Eq. (1) is substituted for Eq. (3), the result is:

$$\eta_c = F_R\left[\alpha\tau - U_L\frac{(T_{ci}-T_a)}{I_t}\right] \quad (4)$$

Because FR, UL, and α τ are all constants,

$$\eta_c \propto \frac{(T_{ci}-T_a)}{I_t} \quad (5)$$

The collector performance coefficient is defined as (Tci – Ta)/It. The performance of the system is anticipated in the theoretical analysis through resolving mathematical equations and adjusting the values of next parameters: temperature of the ambient air (Ta), the temperature of the collector inlet liquid (Tci), and solar irradiation (I_t).

2.3. Dynamic Simulation process in MATLAB program

The following equations models can be utilized in a simple simulation: Equations 6, 7, 8, and 9 may be used to compute the collecting fluid output temperature of flat plate solar collectors:

$$T_{fo} = T_{fi} + \frac{Q_u}{\dot{m}C_{pf}} \quad (6)$$

$$Q_u = A_c F_R[\tau\alpha\, I_t - U_L(T_{fi} - T_a)] \quad (7)$$

$$F_R = \frac{\dot{m}C_{pf}}{A_c U_L}\left(1 - e^{\frac{-A_c U_L F'}{\dot{m}C_{pf}}}\right) \quad (8)$$

$$\eta_c = \frac{Q_u}{A_c I_t} \quad (9)$$

Correlation for(U_t):

[17] Derived a correlation for U_t as since the process to evaluate U_t is laborious and involves an iterative approach.

$$U_t = \left[\frac{N}{\frac{C}{T_{p,m}}\left[\frac{(T_{p,m}-T_a)}{(N+f)}\right]^e} + \frac{1}{h_w}\right]^{-1} + \frac{\sigma(T_{p,m}+T_a)(T_{p,m}^2 - T_a^2)}{(\varepsilon_p + 0.00591Nh_w)^{-1} + \frac{2N+f-1+0.133\varepsilon_p}{\varepsilon_g} - N} \quad (W/m^2°C) \quad (10)$$

N = the number of glass covers.

$$f = (1 + 0.089h_w - 0.1166h_w\varepsilon_p)(1 + 0.07866N) \quad (11)$$

$$C = 250(1 - 0.000051\beta^2) \quad (12)$$

$$e = 0.43\left(1 - \frac{100}{T_{p,m}}\right) \quad (13)$$

β = tilt angle of the collector in degrees.
T_a = temperature of ambient in K.
$T_{p,m}$ = mean temperature of the plate in K.
h_w = heat transfer coefficient of wind in $W/m^2°C$.

The following is the formula for calculating the plate temperature, T_p, which may

also be equivalent to the mean plate temperature, $T_{p,m}$:[18]

$$T_p = T_{in} + 20℃ = T_{p,m} \quad (14)$$

$$U_b = \frac{1}{R} = \frac{k}{L}\ W/m^{2}℃ \quad (15)$$

$$U_e = \frac{(UA)edge}{A_c} = \frac{\frac{k}{L}\times A_{edge}}{A_c}\ W/m^{2}℃ \quad (16)$$

$$U_L = (U_t + U_b + U_e)\ W/m^{2}℃ \quad (17)$$

Efficiency of the Fin (F):

$$F = \frac{\tanh[m(w-D)/2]}{m(w-D)/2} \quad (18)$$

$$m = \sqrt{\frac{U_L}{k\delta}} \quad (19)$$

The efficiency factor of the collector (F′):

$$F' = \frac{\frac{1}{U_L}}{W\left[\frac{1}{U_L[D+(W-D)F]}+\frac{1}{C_b}+\frac{1}{\pi D_i h_{fi}}\right]} \quad (20)$$

$$C_b = \frac{k_b b}{\gamma} \quad (21)$$

2.4. Optimizing the tilt angle

The flat plate solar collector must be set approximately at right angles to the energy rays during the drying seasons to obtain the extreme solar radiation rays. When a collector is oriented south inside the northern hemisphere, it has superior heat performance whole year [19]. The inclination of the collectors facilitates water drainage and enhances air circulation [20]. The optimization equation for tilt angle is based on a model created by [21] and [22].

$$H_T = (H_b + H_d A_i)R_b + H_b(1 - A_i)\left(\frac{1+\cos\beta}{2}\right)\left[1 + f\sin^3\frac{\beta}{2}\right] + H\left(\frac{1-\cos\beta}{2}\right) \quad (22)$$

(H_b) On a horizontal surface, whole beam radiation is emitted.
(β) The tilt angle of a collector.
(H) On a horizontal surface, Monthly daily solar radiations.
(H_d) Total diffuse radiation on the horizontal surface.
(H_T) On a tilted surface, total solar radiation.
(A_i) is an anisotropic index.

$$A_i = \frac{\bar{H}_b}{\bar{H}_o} \quad (23)$$

f is the beam's square root ratio to total radiation, which is defined as:

$$f = \left(\frac{H_b}{H}\right)^{1/2} \quad (24)$$

The beam component can be found by:

$$H_b = H - H_d \quad (25)$$

R_b is a geometric factor

$$R_b = \frac{\cos(\varphi-\beta)\cos\delta\sin\omega_s' + \left(\frac{\pi}{180}\right)\omega_s'\sin(\varphi+\beta)\sin\delta}{\cos\varphi\cos\delta\sin\omega_s' + \left(\frac{\pi}{180}\right)\omega_s'\sin\varphi\sin\delta} \quad (26)$$

$$\dot{\omega}_s = \min\{\cos^{-1}(-\tan\varphi\tan\beta),\ \cos^{-1}(-\tan(\varphi+\beta)\tan\delta)\} \quad (27)$$

We take the lesser of the two numbers in brackets
(ω_s) Sunset hour angle is given by:

$$\omega_s = \cos^{-1}(-\tan^{-1}\varphi\tan^{-1}\delta) \quad (28)$$

(φ)Latitude .
(δ) declinationAngle .

$$\delta = 23.45\ \sin\left[\frac{360}{365}(284 + n)\right] \quad (29)$$

(n) The number of days in a year

2.5. Setup for the experiment equipment

Figure 2 depicts the top view of the FPSC. A solar collector's absorber steel plate was shaped like a wavy sheet to fit the liquid pipelines and headers in the channels and keep excellent contact with them (Figure. 2). In addition, every pipeline has a length of 1.935 meters, an inner diameter of 12 millimeters, and an outside diameter of 14 millimeters. The pipelines are welded on both ends to the header pipeline, which has an internal diameter of 28 mm, an outside diameter of 28.8 mm, and a length of 834 mm.

Absorber-water pipe organization is put in an internal box, which is then fixed to an exterior box. The area between the inside and outside boxes is insulated with wood chips. The front side of a box is at that time enclosed with 5 millimeters of abundant strong basic glass, as well as the air cavity among a plate and a glass cover is 50 millimeters. The total dimension of the FPSC is (1935 x 934 x 100) millimeters, and the operational glazing area is equal to 1.80 m^2. An absorbent surface was coated with nonglossy black to boost the amount of absorbed energy. Figure 3 depicts the practical arrangement of the (FPSC). A K-type thermometer with standard accuracy limits of 97.4% was used to measure the air temperature, the water temperature within the tank, as well as the collector's input and outflow water temperatures.

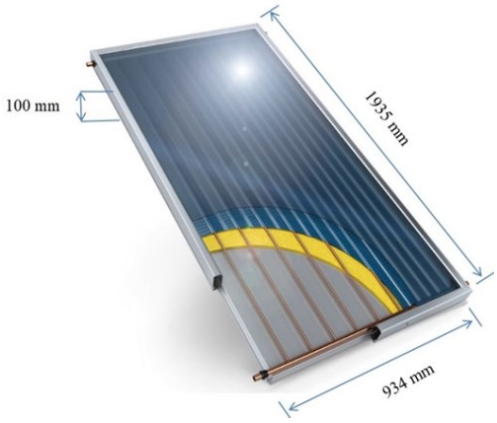

Fig.2 Shows a top view of flat plate solar collector

Also, it has a water flow sensor capacity of 1–30 L/min (type YF-S201). The usual case fluid flow rate with error margins of 3.4%. The solar radiation was measured using a LI-19 read-out device and a data historian with µV sensitivity and basic accuracy of 99 %.

The study was conducted for 30 days during September and October 2021, and a reading was taken every 7 hours between 9 am - 4 pm daily. Water is supplied to the collector from the lowest storage tank level. The realized inlet temperature of the water varies between 25 and 60 °C. The gathered data was utilized to derive system achievement characteristics using the above-mentioned formulae.

Figure 4 shows the general block diagram of the simulation of the flat plate solar collector system in MATLAB program.

Fig. 3 Shows the practical system of the water-heating solar system.

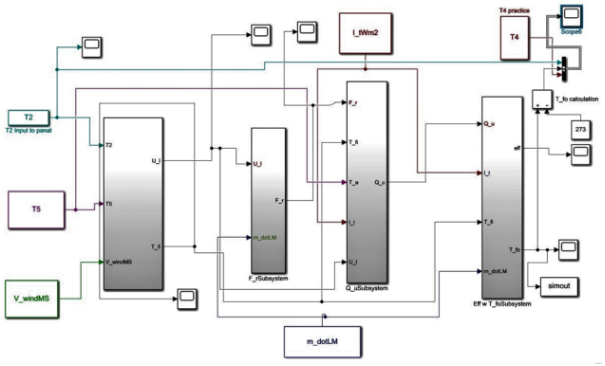

Fig.4. Illustrates simulation of the flat plate solar collector system in MATLAB program general block diagram

In this modeling, the equations of solar panels in previous sections are implemented as mathematical blocks. The inputs of this representation are ambient temperature, wind speed, water mass flow rate, temperature of the collector inlet liquid, and average solar irradiance. These inputs are used to simulate the system. The outputs are the outlet temperature of the panel and efficiency. The curves in the next section are obtained from this model.

Thus, to increase efficiency, five variables were manipulated separately to predict the best operating point of the system. As mentioned previously, this block diagram representation is the dynamic behavior in a continuous time base system.

In this paper, the well-known book in the control engineering field provided by [11] is used as the reference for building, simulating, and optimizing the solar collector panel process

After calibrating the system's instruments, the accuracy of different apparatuses and their errors are attached in Table 1a.

Table 1a: Accuracy of the different apparatuses and their errors.

Device	Accuracy%	Error Rate%
Flow meter	96.6	3.4
Pyranometer	99	1
Anemometer	96	4
Temperature Sensitive	97.4	2.6

3. RESULT AND DISCUSSION

The current parametric paper is based on climatological data for Erbil, the capital of Iraqi Kurdistan. The latitude of Erbil is (36.2191113), and the longitude is (44.009167), during October 2021 (14-Oct). Hourly solar radiation at a particular date and ambient temperature shown in figure 5 were considered constant in the dynamic simulation and optimization. Table 1b displays the parameters that are also fixed to obtain the dynamic simulation with optimization. The collector efficiency, top loss coefficient, heat rate, and fluid outlet temperature of the solar collector are recorded.

The following subsections will deal with the main results for simulating the process depicted in figure 4. The responses (or outputs) obtained by simulating the block diagram are solar collector output temperature and efficiency due to manipulating the design variables. The variables are the change in the mass flow rate, wind speed, average solar irradiance, glass layer, tilt angle, diameter of the raiser pipeline, and tube pitch of the solar collectors' system.

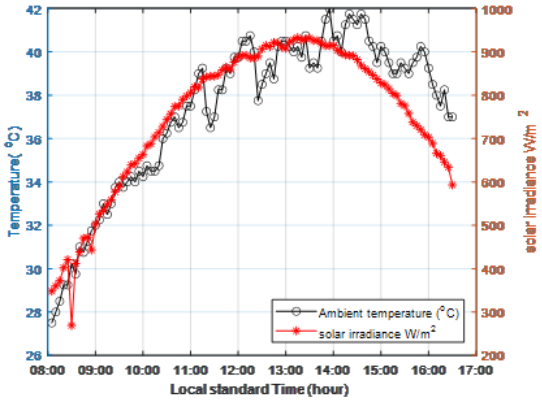

Fig.5 Shows solar irradiance and ambient temperature with Local Standard Time

3.1 Parametric analysis

Dynamic simulation and optimization conducted using different mass flow rates, wind speeds, average solar irradiances, glass layers, diameter of the raiser pipes line, and tube pitch of flat plate solar collectors are shown in figure 7, figure 8, figure 9, figure 10, figure 11, affect to the value of the collector efficiency, top loss coefficient, heat rate, and fluid outlet temperature. In addition, the tilt angle optimization reveals that the only parameter varied is the solar irradiance. Then, this change in the values of the tilt angle is handled to find the best tilt angle, as shown in figure 6. The dynamic simulation and optimization results are discussed in the following subsections.

Table 1b: Illustrates the settings used for adjustment of the dynamic simulation and optimization.

parameters	value
collector Grosses area m^2	1,81
Incline angle	40°
flow rate L/M	2
Thickness of bottom mm	0,40
Absorbances	95%
Emittances	3%
absorber diameter (D) mm	12
Thickness of Absorber mm	0,20
Number of tubes	10
Pitch of tubes (W) mm	86
glass transmittance	91 %
glass thickness mm	4
Thermal conductivity $W/m^2.K$	0.037
wool thickness mm	50
wall thickness of absorber tube mm	0,50
pipe and Absorber material	Copper
average days in the year	228
on a horizontal surface, monthly average daily solar radiation, H Kwh/m^2	7.37
on a horizontal surface diffuse total radiation Hd kwh/m^2	1.474
on a horizontal surface, total beam radiation, Hb kwh/m^2	5.896
Angle of declination	13.56
Latitude φ	36.2191

3.1.1 Tilt angle

Figure 6 and table 2 show plotted values of solar radiation on the collector surface versus the collector's tilt angle, demonstrating that when the collector plate tilt angle was raised from 0°, the solar radiation collected on the collector plate increased significantly. This increase lasted until the tilt angle of the collecting plate reached 30°; after that, any further increase in the tilt angle led to a decrease in the solar energy collected on the collector plate. As a result, 30° was chosen as the best value for the tilt angle of the solar collector plate for the latitude of Erbil (36.2191113) in Iraqi Kurdistan climate conditions, with 27970000 J/m^2/day of solar insolation gathered on the flat plate collector.

Table 2: The outcome of tilt angle optimization

Tilt angle	Solar radiation on Collector surface, ITJ/m^2 .day
0°	26530000
30°	27970000
60°	26410000

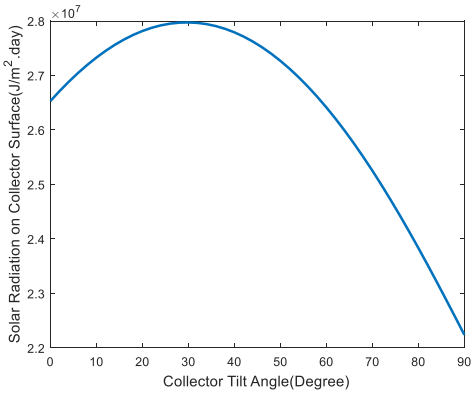

Fig.6 Optimization of tilt angle for the solar collector

3.1.2 Diameter of absorber tube

Table 3 and Figure 7 demonstrate how the collector momentary efficiency varies with collector pipe diameter D and solar radiation intensity. From curves in figure 7, whenever solar radiation intensity is fixed, the collector momentary efficiency improves as the collector tube diameter D increases. Since the pipe diameter D increases, the area of contact between the fluid and tube wall increases. Then, the result of heat transfer will improve. Moreover, increasing the diameter increases the outer surface area of the tube. Hence, the effective absorber area is increased, allowing the fluid to absorb more heat. However, the collector momentary efficiency increases with increasing collector tube diameter under high solar radiation intensity. This phenomenon is increasingly visible.

The results show that the collector momentary efficiency improves as the collector tube diameter D increases from 1 mm to 50 mm under various solar radiation intensities (the fixed values are 450 W/m^2, 650 W/m^2, and 1050 W/m^2 respectively); the efficiency is increased by 1.68%, 1.83%, and 1.96% respectively. Thus, raising the collector pipe diameter D under higher solar radiation intensity may increase the collector's momentary efficiency. Similarly, when the diameter of the collector pipe D is increased from 1 mm to 50 mm, the collector's momentary efficiency under fixed solar radiation intensities is increased from 60.70% to 62.38%, from 66.00% to 67.83%, from 70.54% to 72.50% respectively.

Table 3: Efficiency changes with Solar Irradiance and collector tube diameter

Solar Irradiance w/m^2	Maximum Collector efficiency (%)
450	62.38
650	67.83
1050	72.50

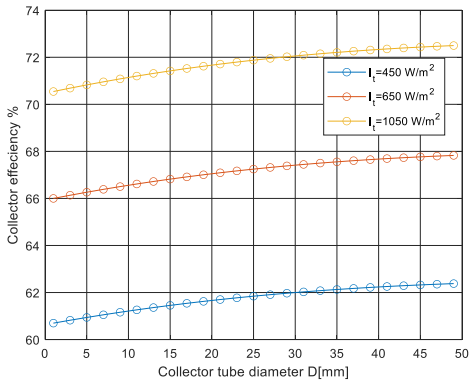

Fig.7 Dynamic simulation and optimizations for the diameter of tube with various solar radiation intensities

3.1.3 Collector tube spacing (W)

Figure 8 and Table 4 show how the collector's momentary efficiency varies with collector pipe spacing (W); under fixed solar radiation intensities for each curve. In any curve, the collector momentary efficiency drops as the collection pipe spacing (W) increases, and vice versa. Consequently, enhance the heat transfer area as well as a weakening of the heat transfer when the collector pipe spacing W is increased. Furthermore, since the usable energy obtained by the working fluid in the tube is smaller than some percentage of the overall energy gained by the absorber plate, the collector momentary efficiency is lowered.

Also, it is observed that the amount of solar radiation is intense, and it is similar to lower the collector momentary efficiency by increasing the collection pipe separation. While, as collector pipe spacing W rises from 86 mm to 186 mm, the collector instantaneously efficiency under similar solar radiation amounts (equals to 450 W/m^2, 650 W/m^2, and 1050 W/m^{2,} respectively) is decreased by 7.84%, 8.53%, and 9.47% respectively.

As a result, the collector momentary efficiency may be significantly improved by lowering the collector pipe spacing W. When the collector tube spacing W is increased from 86 mm to 186 mm, the collector instant efficiency is reduced from 61.31% to 53.47%, 66.07% to 58.14%, and 71.26% to 62.17%, respectively, under various solar radiation intensity levels (450 W/m^2, 650 W/m^2, and 1050 W/m^2).

Table 4: Efficiency changes with Solar Irradiance and collector tube spacing

Solar Irradiance w/m^2	Maximum Collector efficiency (%)
450	61.31
650	66.67
1050	71.26

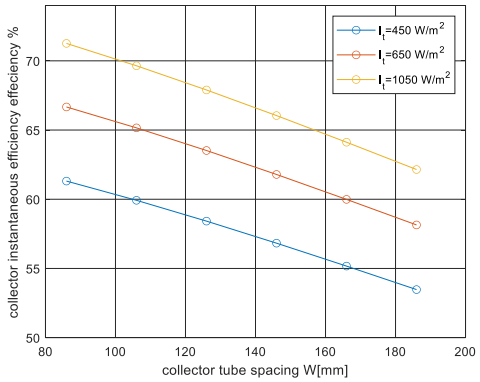

Fig.8 Dynamic simulation and optimizations for the collector tube spacing with solar radiation intensities

3.1.4 the number of glass covers

Figure (9a) and table 5 illustrate that the efficiency increases with increasing the glass cover numbers. This improvement is due to more heat gain. It can be noted that the collector efficiency percentage is about 0.83% in triple glazing, 0.81% in double glazing, and 0.80% in single glazing. Therefore, single glazing has a larger top-loss heat transfer coefficient, lower heat transfer rate to liquid, and lower efficiency.

Then, figure (9b) curves depict the top losses in heat transfer coefficients of single, double, and triple glazing systems shown with time. Many factors influence the total top-loss heat transfer coefficient, including wind, sun intensity, and the space between the absorber plate and the glass cover numbers (i.e., 1 and 2 or 3). In single glazing, the influence of wind velocity and total top loss coefficient is greater than for double and triple glazing systems. Since the temperature differential (ΔT) between the absorber plates and covers (2 or 3) was lower in multi-glass systems, the overall convective heat transfer coefficient was lower, as observed.

Furthermore, referring to figure (9c), the results indicate that its usable heat gain (Q_u) for double and triple glazing is greater than for single glazing. In this case, the upper heat loss coefficient is lower for double and triple glazing. In addition, the heat has been converted properly and transferred to the water. Accordingly, there is more useful and valuable gain absorbed in double glazing compared to single glazing.

Later, figure (9d) depicts the outlet heated water temperature was 343 K for triple glazing. This increase in temperature is due to the influence of distance and double glazing. However, with the same sun intensity, spacing dimensions, and testing circumstances, only 340 k was attained in a single glazing system.

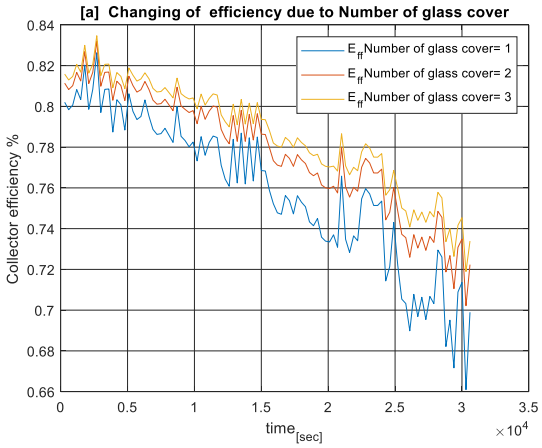

Fig.9 [a] Changing of collector efficiency with time due to the number of glass covers

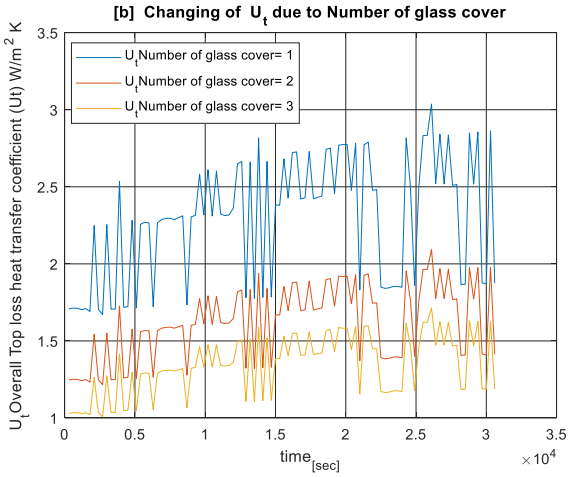

Fig.9 [b] Changing of U_t due to the number of glass covers

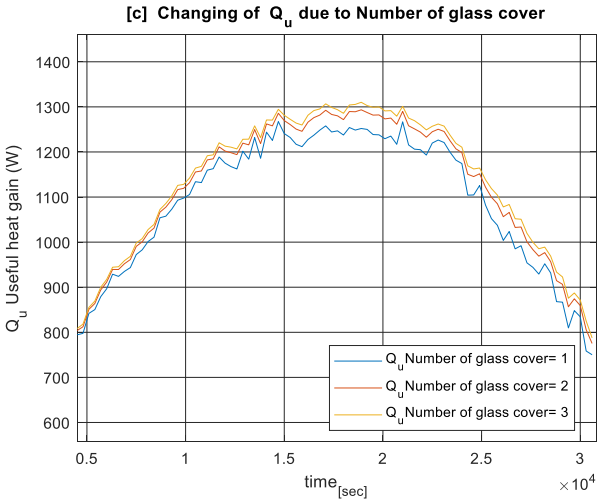

Fig.9 [c] Changing of Q_u with time due to the number of glass covers

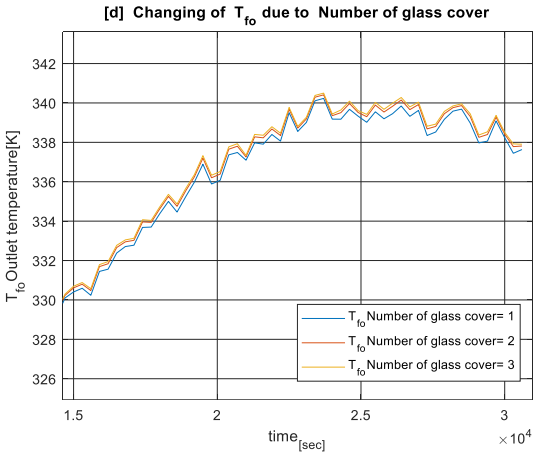

Fig.9 [d] Changing of T_{fo} with time due to the number of glass covers

Table 6 and Figure (10a) demonstrate the escalation of the efficiency with increasing the water flow rate. The increasing flow rate leads to increased thermal energy absorption, improves collector efficiency, and reduces radiation loss.

In the case of 1 L/m, the minimum efficiency gained is 0.64%, while the highest efficiency obtained in the case of 5 L/m is 83%. The fluid with the largest mass flow rate (5 L/m) has the maximum efficiency over time. This increase in efficiency by raising the fluid mass flow rate is due to an increase in the fluid's usable heat gain and improved collector efficiency. The outcome here, the fluid with the smallest flow rate (1 L/m) kg/s has the lowest efficiency compared to the other flow rates in the curve.

3.1.5 Mass flow rate

Table 5: Dynamic simulation and optimizations for the number of glass covers

Number of glass covers	Collector efficiency (%)			Overall top loss w/m2 k			Heat rate (W)			Fluid outlet temperature(K)		
	min	mean	max	min	mean	max	min	mean	max	min	mean	max
1	0.66	0.75	0.80	1.67	2.29	3.03	399	1027	1267	305	327	340
2	0.70	0.77	0.81	1.21	1.62	2.09	402	1054	1294	305	327	341
3	0.71	0.78	0.83	1.00	1.34	1.71	404	1066	1310	305	328	343

Moreover, Table 6 and Figure (10b) show the progression of the water outlet temperature gradient over time for various mass flow rates. It indicates that the temperature of the fluid outflow rises with time and falls with a reduced mass flow rate. In the case of 5 L/m, the lowest fluid outlet temperature attained is 303 K, whereas the highest in the case of 1 L/m is 348 K. Since the mass flow rate of water is inversely related to fluid outlet temperature, a low mass flow rate results in a higher water outlet temperature level. Furthermore, during the slow liquid circulation through the pipe, it needs more time for the water to heat up (homogeneous heat transfer). The temperature rise via the collection also reduces as the water flow rate rises. This drooping in the collector outlet temperatures is a commensurate increase in the usable energy gain and will result in fewer losses.

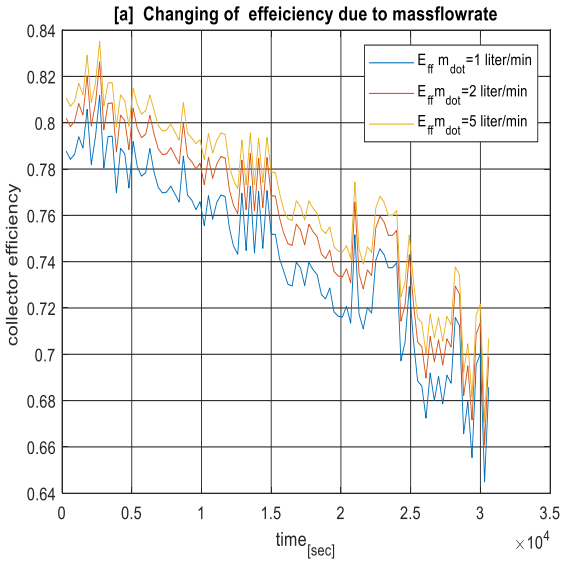

Fig.10 [a] Changing of collector efficiency with time due to mass flow rate

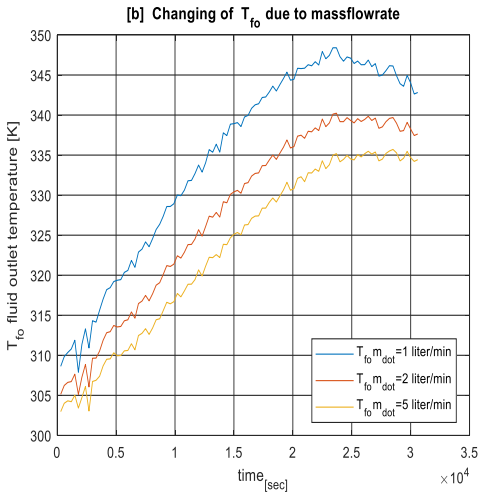

Fig. 10 [b] Changing of T_{fo} with time due to various mass flow rates

Table 6: Result of the dynamic simulation and optimizations for the mass flow rates

Mass flow rate L/min	Collector efficiency (%)			Fluid outlet temperature (K)		
	min	mean	max	min	mean	Max
1	0.64	0.74	0.81	307	334	348
2	0.66	0.75	0.82	305	327	340
5	0.67	0.76	0.83	303	323	335

3.1.6 Wind speed

Figure 11 and Table 7 show the influence of wind speed on the collector's upper heat loss coefficient. The convection heat transfer coefficient rises with wind speed; therefore, the quantity of top heat loss coefficient increases proportionally. The simulation curves reveal that as wind speed increases from 1 m/s to 5 m/s, the upper heat loss coefficient increases by about 50%. For example, when the wind speed is 1 m/s, the maximum peak heat loss coefficient is 2.593 W/m^2K. Whereas at the wind speed of 5 m/s, the maximum peak heat loss coefficient is 3.718 W/m^2K. This behavior is due to increases in wind speed that result in raises in the Raynaud number. Then, it changes the quality of cooling from natural to forced cooling. Hence, a dispersion of the sun rays falling on the collector's surface will happen, in addition to a quick temperature reduction and increased heat loss.

Table 7: Result of the dynamic simulation and optimizations for the wind speed

Wind speed m/s	Top heat loss coefficient of the collector (W/m^2K)		
	min	mean	max
1	2.225	2.393	2.593
3	2.753	2.988	3.302
5	3.057	3.357	3.718

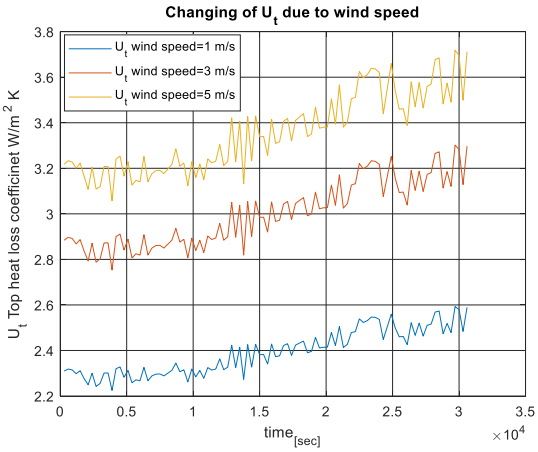

Fig. 11 Dynamic simulation and optimizations for wind speed

3.2 Explain the difference between theoretical and practical outcomes.

The most important parameters to be compared in this study are efficiency and outlet water temperature. The result showed that under the same operating conditions, mainly at maximum values of both, theoretically are 0.82% and 340.2 K, and practically are 0.77%, and 336.9 K, respectively. These minor differences are due to the instability of the surrounding environment in practical tests.

3.3 Current results and published data

In this work, the results can be summarized to confirm the validity; the results are very close to the published results in this scope. The two important parameters, efficiency and outlet water temperature, are improved to justify this research. The improvements rely on deploying different parameters to attain good performances. For this purpose, the modeling of the process is built, simulated, and optimized by MATLAB software. Finally, theoretical and practical results show that they are very close to each other.

3.4 Description of the proposed system

This paper proposed specific flat-plate solar collector systems. Then, the most important parameters are optimized for the flat plate solar collector system. This optimization gives sufficient output values for efficiency and temperature.

The ability of the collector area to heat water (1 m^2) provides 50 liters of hot water per day.

Active system with a mass flow rate not less than 2 L/m.

Triple or double glasses are covered.

The absorber tube's diameter must not be less than 15 mm.

Tube pitch must not exceed 86 mm.

As much as possible, stay away from high wind speeds.

Keep the system clean, particularly the glass cover.

4. CONCLUSION

A mathematical block diagram representation model with simulation is created in the MATLAB environment. Also, different parameters are manipulated and compared to optimize the outputs. The thermal performance of flat plate solar collectors was analyzed based on these parameters. As a result, in the current study following conclusions have been achieved:

1- The collector efficiency was increased from 62.17% to 71.26% when the collector pipe spacing was reduced from 186 mm to 86 mm; lowering collector tube spacing is a good way to boost collector instantaneous efficiency.

2- The efficiency increased by approximately 2% as the collector pipeline diameter grew from 1 mm to 50 mm; increasing the collector pipe diameter is a good way to boost immediate collector efficiency.

3- The optimum efficiency was achieved with triple glazing. It was about 0.83% and the maximum output temperature was 343 k for a triple glazing system while only 340 k for a single glazing system.

4- Increasing the mass flow rate (1 to 5 liters per minute) would improve the system's efficiency from 64% to 83%; also, the highest outflow temperature was 348 k for a mass flow rate of 1 L/M., but only 335 k for a mass flow rate of 5 L/M.

5- Heat loss coefficient rises by around 50% when wind speed is increased from 1 m/s to 5 m/s

6- The best tilt angle for the flat plate solar collector was 30°, biased from the horizontal towards the south, in the examined geographical region (Erbil).

7- Optical efficiency is achieved when the fluid input temperature matches the ambient temperature.

8- The collector efficiency and fluids output temperature are used to understand the final data. It is expected to have 77% efficiency and a fluid output temperature of 60 to 62.5 °C.

9- The use of dynamic investigation (modeling) with actual data will assist the researcher in improving the performance of the solar water flat plate collector.

Recommendation

To be brief, the following things must be understood and taken into account to obtain the best results when using flat plate solar collectors:

As solar irradiation rises, thermal efficiency rises as well.

As the mass flow rate increases, the solar collector's efficiency increases.

Optical efficiency is reached when the fluid intake temperature equals the ambient temperature.

As the ambient temperature and wind speed rise, the energy available for use (heat gain) rapidly decreases.

REFERENCES

[1] C. Kim, "A review of the deployment programs, impact, and barriers of renewable energy policies in Korea," Renewable and Sustainable Energy Reviews, vol. 144, p. 110870, 2021.

[2] S. A. Kalogirou, "Solar thermal collectors and applications," Progress in energy and combustion science, vol. 30, no. 3, pp. 231-295, 2004, doi: http://dx.doi.org/10.1016/j.pecs.2004.02.001.

[3] K. K. F. Rashid, I. I. A. Hamakhan, and C. C. H. Mohammed, "Tilt Angle Optimization and Investigation of the Behavior of a Flat Plate Solar Collector Using MATLAB for Kurdistan Climate Conditions-Iraq," International Journal of Heat and Technology, vol. 40, no. 2, pp. 583-591, 2022, doi: http://dx.doi.org/10.18280/ijht.400227.

[4] S. Mekhilef, R. Saidur, and A. Safari, "A review on solar energy use in industries," Renewable and sustainable energy reviews, vol. 15, no. 4, pp. 1777-1790, 2011, doi: http://dx.doi.org/10.1016/j.rser.2010.12.018.

[5] A. Sözen, T. Menlik, and S. Ünvar, "Determination of efficiency of flat-plate solar collectors using neural network approach," Expert Systems with Applications, vol. 35, no. 4, pp. 1533-1539, 2008, doi: http://dx.doi.org/10.1016/j.eswa.2007.08.080.

[6] H. Dagdougui, A. Ouammi, M. Robba, and R. Sacile, "Thermal analysis and performance optimization of a solar water heater flat plate collector: application to Tétouan (Morocco)," Renewable and Sustainable Energy Reviews, vol. 15, no. 1, pp. 630-638, 2011.

[7] A. M. Do Ango, M. Médale, and C. Abid, "Optimization of the design of a polymer flat plate solar collector," Solar Energy, vol. 87, pp. 64-75, 2013, doi: http://dx.doi.org/10.1016/j.solener.2012.10.006.

[8] P. Cooper, "The effect of inclination on the heat loss from flat-plate solar collectors," Solar Energy, vol. 27, no. 5, pp. 413-420, 1981, doi: http://dx.doi.org/10.1016/0038-092X(81)90006-2.

[9] S. Agbo and E. Okoroigwe, "Analysis ofThermal Losses in the Flat-Plate Collector of a Thermosyphon Solar Water Heater," Research journal of Physics, vol. 1, no. 1, pp. 35-41, 2007.
[10] J. Ma, W. Sun, J. Ji, Y. Zhang, A. Zhang, and W. Fan, "Experimental and theoretical study of the efficiency of a dual-function solar collector," Applied Thermal Engineering, vol. 31, no. 10, pp. 1751-1756, 2011.
[11] K. Ogata, Discrete-time control systems. Prentice-Hall, Inc., 1995.
[12] E. Amer, J. Nayak, and G. Sharma, "Transient method for testing flat-plate solar collectors," Energy Conversion and Management, vol. 39, no. 7, pp. 549-558, 1998, doi: http://dx.doi.org/10.1016/S0196-8904(97)10014-0.
[13] W. Kong et al., "An improved dynamic test method for solar collectors," Solar Energy, vol. 86, no. 6, pp. 1838-1848, 2012.
[14] R. Tang, Y. Cheng, M. Wu, Z. Li, and Y. Yu, "Experimental and modeling studies on thermosiphon domestic solar water heaters with flat-plate collectors at clear nights," Energy Conversion and Management, vol. 51, no. 12, pp. 2548-2556, 2010, doi: http://dx.doi.org/10.1016/j.enconman.2010.04.015.
[15] B. O. Bolaji, "Exergetic analysis of solar drying systems," 2011, doi: http://dx.doi.org/10.4236/nr.2011.22012.
[16] B. O. Bolaji, "Flow design and collector performance of a natural circulation solar water heater," 2006.
[17] J. A. Duffie, W. A. Beckman, and N. Blair, Solar engineering of thermal processes, photovoltaics and wind. John Wiley & Sons, 2020.
[18] I. Ajunwa, D. Yawas, D. Kulla, and I. U. Ibrahim, "Thermal Performance Optimization of Flat Plate Solar Collector using MATLAB," Jurnal Mekanikal, 2020.
[19] S. Abubakar, S. Umaru, M. Kaisan, U. Umar, B. Ashok, and K. Nanthagopal, "Development and performance comparison of mixed-mode solar crop dryers with and without thermal storage," Renewable energy, vol. 128, pp. 285-298, 2018, doi: http://dx.doi.org/10.1016/j.renene.2018.05.049.
[20] B. O. Bolaji and A. P. Olalusi, "Performance evaluation of a mixed-mode solar dryer," 2008.
[21] D. Reindl, W. Beckman, and J. Duffie, "Evaluation of hourly tilted surface radiation models," Solar energy, vol. 45, no. 1, pp. 9-17, 1990, doi: http://dx.doi.org/10.1016/0038-092X(90)90061-G.
[22] Y.-D. Kim, K. Thu, H. K. Bhatia, C. S. Bhatia, and K. C. Ng, "Thermal analysis and performance optimization of a solar hot water plant with economic evaluation," Solar energy, vol. 86, no. 5, pp. 1378-1395, 2012, doi: https://doi.org/10.1016/j.solener.2012.01.030.

Nomenclature

Symbol	Description
FPSC	Flat plate solar Collector
FR	Collector heat removal factor.
Ac	Collector area m^2.
It	Incident tatal solar irradiation W/m^2.
UL	Top heat loss overall $W/m^2°C$.
α	Absorptance.
τ	Transmittance.
Tci	Collector water temperature at inlet °C.
Ta	Temperature of ambient °C.
β	Tilt angle of the collector in degrees.
$T_{p,m}$	Mean temperature of the plate in K.
hw	Heat transfer coefficient of wind in $W/m^2°C$.
η_c	Collector efficiency.
F	Efficiency of the fin.
n	The number of days in a year
φ	Latitude.
δ	declination angle.
F′	Efficiency factor of the collector.
N	The number of glass covers.
Ut	Overall heat loss $W/m^2°C$.

المحاكاة الديناميكية والتحسين الأمثل لمعلمات مجمعات الألواح الشمسية المسطحة باستخدام برنامج MATLAB للظروف المناخية في أربيل- العراق

كامران فتاح رشيد **إدريس عزت حمه خان**
engkamaranmec@gmail.com idres.hamakhan@su.edu.krd
چەلەنك حمەرشيد محمد
chalang.mohammed@su.edu.krd
قسم ميكانيك و ميكاترونيكس - كلية الهندسة - جامعة صلاح الدين – اربيل - العراق

الملخص

يهدف هذا البحث إلى معرفة تأثير معدل تدفق الكتلة وزاوية الميل والإشعاع الشمسي الكلي وحجم الأنابيب وعدد الأغطية الزجاجية على أداء مجمع المياه بالطاقة الشمسية. تم إنشاء منصة الاختبار لجمع البيانات عن شهري سبتمبر وأكتوبر بالكامل واستخدامها كنقطة محورية لتحليل أداء نظام تسخين المياه بالطاقة الشمسية. تم تطبيق المحاكاة الديناميكية والتحسين باستخدام برنامج MATLAB *على البيانات العملية بدلاً من حساب متوسط البيانات لاستقصاء أداء* SWHS. *هذه هي المرة الأولى التي يستخدم فيها المؤلفون البيانات العملية بالكامل بدلاً من استخدام المتوسط لتقريب التحقيق الديناميكي النظري لمجمع الألواح الشمسية المسطحة. كانت الإنجازات على النحو التالي: زيادة في كفاءة المجمع من 62.17٪ إلى 71.26٪ عندما تم تقليل التباعد بين أنابيب المجمع من 186 ملم إلى 86 ملم. كانت الزيادة في الكفاءة حوالي 2٪ حيث نما قطر خط أنابيب المجمع من 1 مم إلى 50 مم ؛ تم تحقيق الكفاءة المثلى مع الزجاج الثلاثي وكانت حوالي 0.83٪؛ ستؤدي زيادة معدل التدفق (1 إلى 5 لترات في الدقيقة) إلى تحسين كفاءة النظام من 64٪ إلى 83٪. كانت أفضل زاوية ميل لمجمع الألواح الشمسية المسطحة 30 درجة ، كما أن معامل فقدان الحرارة يرتفع بحوالي 50٪ عند زيادة سرعة الرياح من 1 م / ث إلى 5 م / ث. إن استخدام الاستقصاء الديناميكي مع البيانات الفعلية سيساعد الباحث في تحسين أداء مجمّع الألواح الشمسية المسطحة للمياه. تعرض هذه الدراسة لأول مرة في العراق - أربيل تحسين مجموعة من أهم المعلمات لنظام تجميع الطاقة الشمسية المسطحة ، والتي بدورها تؤثر على تحسين أداء هذا النظام.*

الكلمات الداله :

محاكاة ديناميكية ، طاقة شمسية ، كفاءة المجمع ، تحليل الأداء.